

Patterns formation in axially symmetric Landau-Lifshitz-Gilbert-Slonczewski equations

June 7, 2019

C. Melcher¹ & J.D.M. Rademacher²

Abstract

The Landau-Lifshitz-Gilbert-Slonczewski equation describes magnetization dynamics in the presence of an applied field and a spin polarized current. In the case of axial symmetry and with focus on one space dimension, we investigate the emergence of space-time patterns in the form of coherent structures, whose profiles asymptote to wavetrains. In particular, we give a complete existence and stability analysis of wavetrains and prove existence of various coherent structures, including soliton- and domain wall-type solutions. Decisive for the solution structure is the size of anisotropy compared with the difference of field intensity and current intensity normalized by the damping.

1 Introduction

This paper concerns the analysis of spatio-temporal pattern formation for the axially symmetric Landau-Lifshitz-Gilbert-Slonczewski equation in one space dimension

$$\partial_t \mathbf{m} = \mathbf{m} \times \left[\alpha \partial_t \mathbf{m} - \partial_x^2 \mathbf{m} + (\mu m_3 - h) \hat{\mathbf{e}}_3 + \beta \mathbf{m} \times \hat{\mathbf{e}}_3 \right] \quad (1)$$

as a model for the magnetization dynamics $\mathbf{m} = \mathbf{m}(x, t) \in \mathbb{S}^2$ (i.e. \mathbf{m} is a direction field) driven by an external fields $\mathbf{h} = h \hat{\mathbf{e}}_3$ and currents $\mathbf{j} = \beta \hat{\mathbf{e}}_3$. The parameters $\alpha > 0$ and $\mu \in \mathbb{R}$ are the Gilbert damping factor and the anisotropy constant, respectively. A brief overview of the physical background and interpretation of terms is given below in Section 2. While the combination of field and current excitations gives rise to a variety of pattern formation phenomena, see e.g. [4, 11, 12, 15], not much mathematically rigorous work is available so far, in particular for the dissipative case $\alpha > 0$ that we consider. The case of axial symmetry is not only particularly convenient from a technical perspective. It offers at the same time valuable insight in the emergence of space-time patterns and displays strong similarities to better studied dynamical systems such as real and complex Ginzburg-Landau equations. In this framework we examine the existence and stability of wavetrain solutions of (1), i.e., solutions of the form

$$\mathbf{m}(x, t) = e^{i\varphi(kx - \omega t)} \mathbf{m}_0,$$

where the complex exponential acts on $\mathbf{m}_0 \in \mathbb{S}^2$ by rotation about the $\hat{\mathbf{e}}_3$ -axis (cf. Figure 1 for an illustration). We give a complete characterization of wavetrains and their L^2 -stability. We also investigate the existence of their spatial connections, i.e. coherent structures of the form

$$\mathbf{m}(x, t) = e^{i\varphi(x, t)} \mathbf{m}_0(x - st) \quad \text{where} \quad \varphi(x, t) = \phi(x - st) + \Omega t$$

¹Lehrstuhl I für Mathematik and JARA-FIT, RWTH Aachen University, 52056 Aachen, Germany, melcher@rwth-aachen.de

²Fachbereich 3 – Mathematik, Universität Bremen, Postfach 33 04 40, 28359 Bremen, Germany, rademach@math.uni-bremen.de

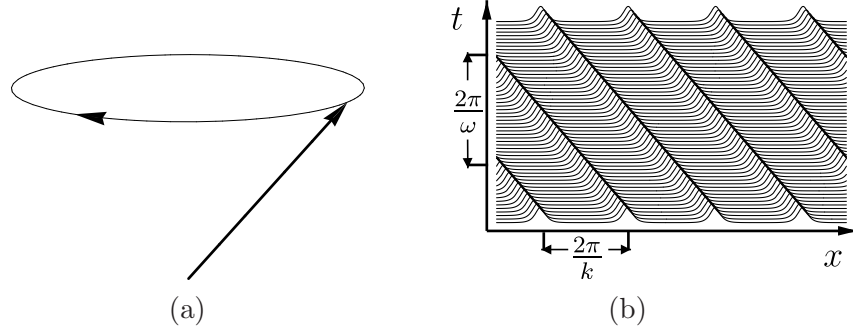


Figure 1: Illustration of a wavetrain profile $\mathbf{m}(\varphi)$ (a) in the 2-sphere and (b) as a space-time plot of, e.g., m_2 . In (a) the thick arrow represents $\mathbf{m} = (m, m_3)$, the thin line its trajectory as a function of $\varphi = kx - \omega t$.

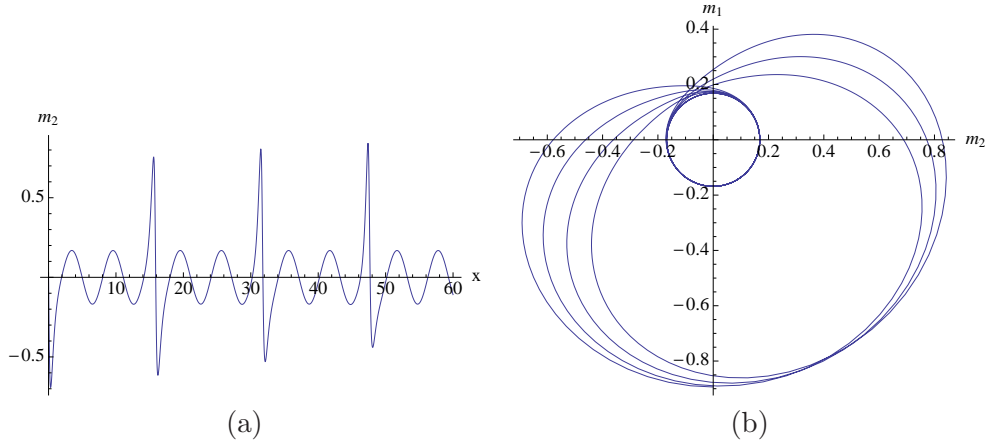


Figure 2: Part of a coherent structure profile for supercritical anisotropy in spherical coordinates. In the reduced equations (32) it maps to a long period solution. Here $\mu = 7$, $h - \Omega = -1$, $\Omega = \beta/\alpha$ and first integral $C = 1$, cf. (31). (a) $m_2(x)$, (b) (m_1, m_2) -plane.

and such that $\mathbf{m}_0(\xi) = (\sin \theta(\xi), 0, \cos \theta(\xi))$. We completely characterize the existence of stationary ($s = 0$) and small amplitude coherent structures with $|s|$ above an explicit threshold, and identify fast ($|s| \gg 1$ larger than an abstract threshold) coherent structures. The analysis bears similarities with that of the real Ginzburg-Landau equation, which we also briefly discuss.

The small amplitude and fast coherent structures are forms of magnetic domain walls, with the spatially asymptotic states being the constant up- or down-magnetization states ($\mathbf{m} = \pm \hat{\mathbf{e}}_3$), or a wavetrain. The connections with the wavetrain thus form a spatial interface between constant and precessional states.

More specifically, the parameter space for existence of wavetrains and coherent structures is largely organized by the difference of anisotropy μ and the force balance $|h - \beta/\alpha|$, of magnetic field strength minus the ratio of current intensity and damping factor, which also appears in the ODE for solutions that are homogeneous in space. Motivated by the nature of bifurcations we introduce the following notions:

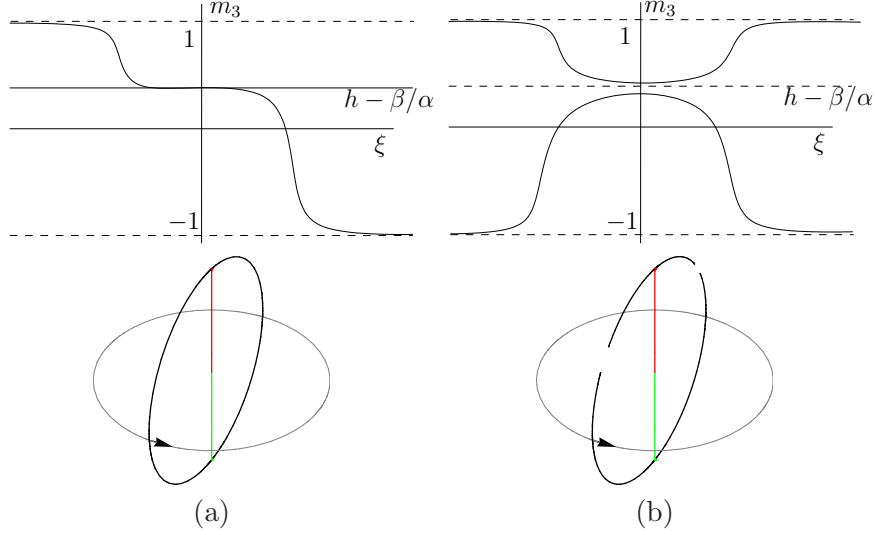


Figure 3: Upper row: Superimposed snapshots of homogeneous ($d\phi/d\xi = q = 0$) coherent structure profiles for supercritical anisotropy. Compare Figure 7(a). Bottom row: Ranges of these profiles in the sphere, which rotate in time with frequency $\Omega = \alpha/\beta$, about the \hat{e}_3 -axis (black arrows). (a) Half-period of a profile that crosses $\pm\hat{e}_3$, and passes close to a homogeneous wavetrain, which generates the plateau around $\xi = 0$. (b) superposition of two periodic profiles crossing \hat{e}_3 and $-\hat{e}_3$, respectively.

- ‘supercritical anisotropy’ if $\mu > |h - \beta/\alpha|$
- ‘subcritical anisotropy’ if $0 < |\mu| < |h - \beta/\alpha|$,
- ‘subsubcritical anisotropy’ if $-\mu > |h - \beta/\alpha|$.

From a physical viewpoint μ and α are material specific, while h, β are control parameters.

Notably, supercritical anisotropy is ‘easy-plane’, while subsubcritical anisotropy is ‘easy-axis’ (see §2). In this framework the main results may be summarized somewhat informally as follows:

The homogeneous up- and down-magnetization equilibria $\pm\hat{e}_3$. Both of these are unstable for the supercritical anisotropy, and both are stable in the subsubcritical regime. If $h > \beta/\alpha$ then \hat{e}_3 is unstable for subcritical anisotropy, while $-\hat{e}_3$ is stable, and the situation is reversed for $h < \beta/\alpha$. The transition from sub- to supercritical is a supercritical Turing-type bifurcation, while the transition from sub- to subsubcritical is a subcritical one. (Lemma 1 and Theorem 1.)

Wavetrains.

1. *Supercritical anisotropy:* There exist unique wavetrains for all wavenumbers with absolute value in $[0, \sqrt{\mu - |h - \beta/\alpha|})$ and above $\sqrt{\mu + |h - \beta/\alpha|}$. The only stable wavetrains have wavenumber k near zero and become sideband unstable at a critical wavenumber below $\sqrt{\mu - |h - \beta/\alpha|}$.

2. *Subcritical anisotropy:* There exist unique wavetrains for all wavenumbers larger than $\sqrt{\mu + |h - \beta/\alpha|}$, and these are all unstable.
3. *Subsubcritical anisotropy:* There exist unique wavetrains for all wavenumbers, and these are all unstable.

(Theorems 1, 2)

Stationary coherent structures.

1. *Supercritical anisotropy:* For fixed parameters there exist various stationary coherent structures ($s = 0$) including a class of ‘homogeneous’ ones, whose range lies within a meridian on the sphere that rotates in time azimuthally with constant frequency β/α . An interesting case of the latter is a symmetric pair of ‘phase slip’ soliton-type coherent structures, whose spatially asymptotic states are the same spatially homogeneous oscillation ($k = 0$), but the intermediate profile crosses either \hat{e}_3 or $-\hat{e}_3$, so that the asymptotic states differ azimuthally by 180° . There also exists a non-homogeneous soliton-type solution with asymptotic state being a wavetrain.
2. *Sub- and subsubcritical anisotropy:* All stationary coherent structures have periodic profiles except a homogeneous phase slip soliton to $\pm\hat{e}_3$ for $\text{sgn}(h - \beta/\alpha) = \pm 1$.

(Theorems 3, 4)

Fast and small amplitude coherent structure. For each sufficiently large speed there exist a family of front-type coherent structures parametrized by the azimuthal frequency. Their profiles connect $\pm\hat{e}_3$ with each other or, if it exists, the unique wavetrain. Small amplitude coherent structure above an explicit lower speed bound are of front type and exist only for super- and subcritical anisotropy. (Theorems 5, 6.)

While the stability analysis of wavetrains shows that the fast and small coherent structures are unstable in an L^2 -sense, they could be stable in weighted spaces, and knowing unstable solutions may also be useful for stabilizing control schemes. However, we do not investigate this further here.

Higher space dimensions. In N space dimensions, the second derivative with respect to x in (1) would be replaced by a Laplace operator $\sum_{j=1}^N \partial_{x_j}^2$. Wavetrain type solutions are then of the form

$$\mathbf{m}(x, t) = \mathbf{m}_*(k \cdot x - \omega t),$$

where $k = (k_1, \dots, k_N)$. Notably, for $k_j = 0$, $2 \leq j \leq N$ these are solutions from one space dimension extended trivially (constant) in the additional directions.

Conveniently, the rotation symmetry (gauge invariance in the Ginzburg-Landau context), means that the analyses of $\pm\hat{e}_3$ and these wavetrains is already covered by that of the one-dimensional case: the linearization is space-independent and therefore there is no symmetry breaking due to different k_j . Indeed, all relevant quantities are rotation symmetric, depending only on $k^2 = \sum_{j=1}^N k_j^2$ or $\ell^2 = \sum_{j=1}^N \ell_j^2$, where $\ell = (\ell_1, \dots, \ell_N)$ is the Fourier wavenumber

vector of the linearization. In particular, the only nontrivial stability boundary are sideband instabilities, which occur simultaneously for all directions.

Concerning coherent structures, (27) turns into an elliptic PDE in general so that the analysis in this paper only allows for the trivial extension into higher dimensions.

This article is organized as follows. In Section 2, the terms in the model equation (1) and its well-posedness are discussed. Section 3 concerns the stability of the trivial steady states $\pm \hat{\mathbf{e}}_3$ and in §4 existence and stability of wavetrains are analyzed. Section 5 is devoted to coherent structures.

Acknowledgement. JR has been supported in part by the NDNS+ cluster of the Dutch Science Fund (NWO).

2 Landau-Lifshitz equations

The classical equation of magnetization dynamics, the conservative Landau-Lifshitz equation [16], corresponds to a torque balance for the magnetic moment, represented by a unit vector field $\mathbf{m} = \mathbf{m}(t) \in \mathbb{S}^2$,

$$\dot{\mathbf{m}} + \gamma \mathbf{m} \times \mathbf{h}_{\text{eff}} = 0.$$

It features a free precession of \mathbf{m} about the effective field $\mathbf{h}_{\text{eff}} = -\mathcal{E}'(\mathbf{m})$, i.e., minus the variation of the underlying interaction energy $\mathcal{E} = \mathcal{E}(\mathbf{m})$, which is conserved in time. The gyromagnetic ratio $\gamma > 0$ is a parameter which appears as the typical precession frequency. By rescaling time, one can always assume $\gamma = 1$. Adding a dissipative counter-field, which is proportional to the velocity $\dot{\mathbf{m}}$, yields the Landau-Lifshitz-Gilbert equation (LLG) [9, 13]

$$\dot{\mathbf{m}} = \mathbf{m} \times (\alpha \mathbf{m}_t - \mathbf{h}_{\text{eff}}). \quad (2)$$

The Gilbert damping factor $\alpha > 0$ is a constant that can be interpreted dynamically as the inverse of the typical relaxation time. It is useful to take into account that there are several equivalent forms of LLG. Carrying out another cross multiplication of (2) by \mathbf{m} from the left and taking into account that $-\mathbf{m} \times \mathbf{m} \times \boldsymbol{\xi} = \boldsymbol{\xi} - (\mathbf{m} \cdot \boldsymbol{\xi})\mathbf{m}$ is the orthonormal projection to the tangent plane of \mathbb{S}^2 at \mathbf{m} , one obtains

$$\alpha \dot{\mathbf{m}} + \mathbf{m} \times \dot{\mathbf{m}} = -\mathbf{m} \times \mathbf{m} \times \mathbf{h}_{\text{eff}}, \quad (3)$$

where the right hand side can also be written as $\mathbf{h}_{\text{eff}} - (\mathbf{m} \cdot \mathbf{h}_{\text{eff}})\mathbf{m}$. Multiplying this equation by α and adding it to the original one, one obtains the dissipative Landau-Lifshitz equation³, i.e.

$$(1 + \alpha^2)\dot{\mathbf{m}} = -\mathbf{m} \times (\alpha \mathbf{m}_t + \mathbf{h}_{\text{eff}}), \quad (4)$$

which has been introduced in the original work [16]. In case of LLG, the energy $\mathcal{E}(\mathbf{m})$ is not conserved but a Liapunov functional, i.e., more precisely (recall $\mathbf{h}_{\text{eff}} = -\mathcal{E}'(\mathbf{m})$)

$$\frac{d}{dt}\mathcal{E}(\mathbf{m}(t)) = -\alpha \|\dot{\mathbf{m}}(t)\|^2 \quad \text{or equivalently} \quad \frac{d}{dt}\mathcal{E}(\mathbf{m}(t)) = -\frac{\alpha}{1 + \alpha^2} \|\mathbf{m} \times \mathbf{h}_{\text{eff}}\|^2.$$

Gilbert damping enables the magnetization to approach (spiral down to) a steady state, i.e. satisfying $\mathbf{m} \times \mathbf{h}_{\text{eff}} = 0$ (Browns equation), as $t \rightarrow \infty$.

³original form $\dot{\mathbf{m}} = -\mathbf{m} \times \mathbf{h}_{\text{eff}} - \lambda \mathbf{m} \times \mathbf{m} \times \mathbf{h}_{\text{eff}}$ with Landau-Lifshitz damping $\lambda > 0$

Spin-torque interaction. The system can be driven out of equilibrium conventionally by external magnetic fields \mathbf{h} which appears as part of the effective field. In modern spintronic applications, magnetic systems are excited by spin polarized currents (with direction of polarization $\hat{\mathbf{e}}_p \in \mathbb{S}^2$) giving rise to a spin torque

$$\mathbf{m} \times \mathbf{m} \times \mathbf{j} \quad \text{where} \quad \mathbf{j} = \beta \frac{\hat{\mathbf{e}}_p}{1 + c \mathbf{m} \cdot \hat{\mathbf{e}}_p}, \quad (5)$$

which has been introduced in [1, 24]. Here, the parameters $\beta > 0$ and $c \in (-1, 1)$ depend on the intensity of the current and ratio of polarization [3]. Typically we have $\hat{\mathbf{e}}_p = \hat{\mathbf{e}}_3$. Accordingly, the modified Landau-Lifshitz-Gilbert equation, also called Landau-Lifshitz-Gilbert-Slonczewski equation (LLGS), reads

$$\dot{\mathbf{m}} = \mathbf{m} \times (\alpha \dot{\mathbf{m}} - \mathbf{h}_{\text{eff}} + \mathbf{m} \times \mathbf{j}). \quad (6)$$

One may extend the notion of effective field to include current interaction by letting

$$\mathbf{H}_{\text{eff}} = \mathbf{h}_{\text{eff}} - \mathbf{m} \times \mathbf{j},$$

where the second term is usually called Slonczewski term. In this framework (6) can also be written in the form (3) and (4) with \mathbf{h}_{eff} replaced by \mathbf{H}_{eff} . Observe, however, that the Slonczewski term (and hence \mathbf{H}_{eff}) is non-variational and that the energy is no longer a Liapunov functional. Introducing the potential $\Psi(\mathbf{m}) = \frac{\beta}{c} \ln(1 + c \mathbf{m} \cdot \hat{\mathbf{e}}_p)$ of \mathbf{j} (for $c \neq 0$) reveals the *skew variational* structure

$$\mathbf{m} \times [\alpha \dot{\mathbf{m}} + \mathcal{E}'(\mathbf{m})] = -\mathbf{m} \times \mathbf{m} \times [\dot{\mathbf{m}} + \Psi'(\mathbf{m})].$$

The continuum equation. Continuum theories are concerned with magnetization fields $\mathbf{m} = \mathbf{m}(x, t)$ such that $|\mathbf{m}| = 1$. In the micromagnetic model the underlying interaction energies are integral functionals in \mathbf{m} containing in particular exchange (Dirichlet) interaction, dipolar stray-field interaction, crystal anisotropy and Zeeman interaction with external magnetic field, see e.g. [13]. The effective field is computed from the L^2 gradient of the energy, i.e. $\mathbf{h}_{\text{eff}} = -\nabla_{L^2} \mathcal{E}(\mathbf{m})$, and (6) becomes a partial differential equation. In this paper we shall mainly focus on the spatially one-dimensional situation and consider energies of the form

$$\mathcal{E}(\mathbf{m}) = \frac{1}{2} \int (|\partial_x \mathbf{m}|^2 + \mu m_3^2) dx - \int \mathbf{h} \cdot \mathbf{m} dx. \quad (7)$$

Here, $\mathbf{h} \in \mathbb{R}^3$ is a constant applied magnetic field. The parameter $\mu \in \mathbb{R}$ features *easy plane* anisotropy for $\mu > 0$ and *easy axis* anisotropy for $\mu < 0$, respectively, according to energetically preferred subspaces. This term comprises crystalline and shape anisotropy effects. Shape anisotropy typically arises from stray-field interactions which prefer magnetizations tangential to the sample boundaries. Hence $\mu > 0$ corresponds to a thin-film perpendicular to the $\hat{\mathbf{e}}_3$ -axis whereas $\mu < 0$ corresponds to a thin wire parallel to the $\hat{\mathbf{e}}_3$ -axis. The effective field corresponding to (7) reads

$$\mathbf{h}_{\text{eff}} = \partial_x^2 \mathbf{m} - \mu m_3 \hat{\mathbf{e}}_3 + \mathbf{h}. \quad (8)$$

With the choices $\mathbf{h} = h \hat{\mathbf{e}}_3$ and $\hat{\mathbf{e}}_p = \hat{\mathbf{e}}_3$, the Landau-Lifshitz-Gilbert-Slonczewski equation (6) exhibits the aforementioned rotation symmetry about the $\hat{\mathbf{e}}_3$ -axis. Our analysis is valid for small $|c|$ in (5) and we focus on $c = 0$ so that $\mathbf{j} = \beta \hat{\mathbf{e}}_3$. This is equation (1), i.e.,

$$\partial_t \mathbf{m} = \mathbf{m} \times \left[\alpha \partial_t \mathbf{m} - \partial_x^2 \mathbf{m} + (\mu m_3 - h) \hat{\mathbf{e}}_3 + \beta \mathbf{m} \times \hat{\mathbf{e}}_3 \right].$$

The presence of a spin torque $\mathbf{m} \times \mathbf{m} \times \mathbf{j}$ exerted by a constant current may induce switching between magnetization states or magnetization oscillation, [2, 5, 3]. For the latter effect, the energy supply due to the electric current compensates the energy dissipation due to damping enabling a stable oscillation, called *precessional states*. In applications the typical frequency is in the range of GHz, so that a precessional state would basically act as a microwave generator. In the class of spatially homogeneous states, precessional states are periodic orbits with $m_3 = \text{const.}$ and of constant angular velocity β/α . It is more subtle, however, to understand the occurrence and stability of spatially non-homogeneous precessional states.

Extensions and related work. Non-symmetric variants of our equation (1) have been used e.g. in the description of the field driven motion of a flat domain wall connecting antipodal steady states $m_3 = \pm 1$ as $x_1 \rightarrow \pm\infty$. A prototypical situation is the field driven motion of a flat Bloch wall in an uniaxial the bulk magnet governed by

$$\partial_t \mathbf{m} = \mathbf{m} \times (\alpha \partial_t \mathbf{m} - \partial_x^2 \mathbf{m} + \mu_1 m_1 \hat{\mathbf{e}}_1 + (\mu_3 m_3 - h) \hat{\mathbf{e}}_3).$$

In this case $\mu_1 > 0 > \mu_3$, where μ_1 corresponds to stray-field and μ_3 to crystalline anisotropy. Explicit traveling wave solutions were obtained in unpublished work by Walker, see e.g. [13], and reveal interesting effects such as the existence of a terminal velocity (called Walker velocity) and the notion of an effective wall mass. A mathematical account on Walker's explicit solutions and investigations on their stability, possible extensions to finite layers and curved walls can be found e.g. in [7, 18, 23]. Observe that our axially symmetric model is obtained in the limit $\mu_1 \searrow 0$. On the other hand, the singular limit $\mu_3 \rightarrow +\infty$ leads to trajectories confined to the $\{m_3 = 0\}$ plane (equator map), and can be interpreted as a thin-film limit. In suitable parameter regimes it can be shown that the limit equation is a dissipative wave equation governing the motion of Néel walls [6, 17, 19].

Well-posedness of LLGS. It is well-known that Landau-Lifshitz-Gilbert equations and its variants have the structure of quasilinear parabolic systems. In the specific case of (1), one has the extended effective field $\mathbf{H}_{\text{eff}} = \mathbf{h}_{\text{eff}} - \mathbf{m} \times \mathbf{j}$, more precisely

$$\mathbf{H}_{\text{eff}} = \partial_x^2 \mathbf{m} - f(\mathbf{m}) \quad \text{where} \quad f(\mathbf{m}) = (\mu m_3 - h) \hat{\mathbf{e}}_3 + \beta \mathbf{m} \times \hat{\mathbf{e}}_3. \quad (9)$$

Hence the corresponding Landau-Lifshitz form (4) of (1) reads

$$(1 + \alpha^2) \partial_t \mathbf{m} = -\mathbf{m} \times \left[\partial_x^2 \mathbf{m} - f(\mathbf{m}) \right] - \alpha \mathbf{m} \times \mathbf{m} \times \left[\partial_x^2 \mathbf{m} - f(\mathbf{m}) \right]. \quad (10)$$

Taking into account⁴

$$\mathbf{m} \times \partial_x^2 \mathbf{m} = \partial_x (\mathbf{m} \times \partial_x \mathbf{m}) \quad \text{and} \quad -\mathbf{m} \times \mathbf{m} \times \partial_x^2 \mathbf{m} = \partial_x^2 \mathbf{m} + |\partial_x \mathbf{m}|^2 \mathbf{m} \quad (11)$$

valid for \mathbf{m} sufficiently smooth and $|\mathbf{m}| = 1$, one sees that (10) has the form

$$\partial_t \mathbf{m} = \partial_x (A(\mathbf{m}) \partial_x \mathbf{m}) + B(\mathbf{m}, \partial_x \mathbf{m}) \quad (12)$$

with analytic functions $A : \mathbb{R}^3 \rightarrow \mathbb{R}^{3 \times 3}$ and $B : \mathbb{R}^3 \times \mathbb{R}^3 \rightarrow \mathbb{R}^3$ such that $A(\mathbf{m})$ is uniformly elliptic for $\alpha > 0$, in fact

$$\boldsymbol{\xi} \cdot A(\mathbf{m}) \boldsymbol{\xi} = \frac{\alpha}{1 + \alpha^2} |\boldsymbol{\xi}|^2 \quad \text{for all} \quad \boldsymbol{\xi} \in \mathbb{R}^3.$$

⁴ $-\mathbf{m} \times \mathbf{m} \times \boldsymbol{\xi} = (1 - \mathbf{m} \otimes \mathbf{m}) \boldsymbol{\xi}$ is the orthogonal projection of $\boldsymbol{\xi}$ onto the tangent space $T_{\mathbf{m}} \mathbb{S}^2$ at \mathbf{m} .

Well-posedness results for $\alpha > 0$ can now be deduced from techniques based on higher order energy estimates as in [20, 21] or maximal regularity and interpolation as in [22]. In particular, we shall rely on results concerning perturbations of wavetrains, traveling waves, and steady states. Suppose $\mathbf{m}_* = \mathbf{m}_*(x, t)$ is a smooth solution of (1) with bounded derivatives up to all high orders (only sufficiently many are needed) and $\mathbf{m}_0 : \mathbb{R} \rightarrow \mathbb{S}^2$ is such that $\mathbf{m}_0 - \mathbf{m}_*(\cdot, 0) \in H^2(\mathbb{R})$. Then there exist $T > 0$ and a smooth solution $\mathbf{m} : \mathbb{R} \times (0, T) \rightarrow \mathbb{S}^2$ of (1) such that $\mathbf{m} - \mathbf{m}_* \in C^0([0, T]; H^2(\mathbb{R})) \cap C^1([0, T]; L^2(\mathbb{R}))$ with

$$\lim_{t \searrow 0} \|\mathbf{m}(t) - \mathbf{m}_0\|_{H^2} = 0 \quad \text{and} \quad \lim_{t \nearrow T} \|\mathbf{m}(t) - \mathbf{m}_*(\cdot, t)\|_{H^2} = \infty \quad \text{if } T < \infty.$$

The solution is unique in its class and the flow map depends smoothly on initial conditions and parameters.

Given the smoothness of solutions, we may compute pointwise $\partial_t |\mathbf{m}|^2 = 2\mathbf{m} \cdot \partial_t \mathbf{m}$, so that for $|\mathbf{m}| = 1$ the cross product form of the right hand side of (10) gives $\partial_t |\mathbf{m}|^2 = 0$. Hence, the set of unit vector fields, $\{|\mathbf{m}| = 1\}$, is an invariant manifold of (12) consisting of the solutions to (1) that we are interested in.

In addition to well-posedness, also stability and spectral theory for (12), see, e.g., [22], carry over to (1). In particular, the computations of L^2 -spectra in the following sections are justified and yield nonlinear stability for strictly stable spectrum and nonlinear instability for the unstable (essential) spectrum.

Landau-Lifshitz-Gilbert-Slonczewski versus complex Ginzburg-Landau equations. Stereographic projection of (1) yields

$$(\alpha + i)\zeta_t = \partial_x^2 \zeta - \frac{2\bar{\zeta}(\partial_x \zeta)^2}{1 + |\zeta|^2} + \mu \frac{(1 - |\zeta|^2)\zeta}{1 + |\zeta|^2} - (h + i\beta)\zeta \quad \text{where} \quad \zeta = \frac{m_1 + im_2}{1 + m_3},$$

valid for magnetizations avoiding the south pole.

There is also a global connection between LLG and CGL in the spirit of the classical Hasimoto transformation [10], which turns the (undamped) Landau-Lifshitz equation in one space dimension ($\mathbf{h}_{\text{eff}} = \partial_x^2 \mathbf{m}$) into the focussing cubic Schrödinger equation. The idea is to disregard the customary coordinates representation and to introduce instead a pull-back frame on the tangent bundle along \mathbf{m} . In the case of $\mu = \beta = h = 0$, i.e. $\mathbf{h}_{\text{eff}} = \partial_x^2 \mathbf{m}$, this leads to

$$(\alpha + i)\mathcal{D}_t u = \mathcal{D}_x^2 u \tag{13}$$

where $u = u(x, t)$ is the complex coordinate of $\partial_x \mathbf{m}$ in the moving frame representation, and \mathcal{D}_x and \mathcal{D}_t are covariant derivatives in space and time giving rise to cubic and quintic nonlinearities, see [20, 21] for details.

3 Turing instabilities of the steady states $\mathbf{m} = \pm \hat{\mathbf{e}}_3$

As a starting point and to motivate the subsequent analysis of more complex patterns, let us consider the stability of the constant magnetizations $\pm \hat{\mathbf{e}}_3$. Substituting $\mathbf{m} = \pm \hat{\mathbf{e}}_3 + \delta \mathbf{n} + o(\delta)$, where $\mathbf{n} = (n, 0) \in T_{\mathbf{m}} \mathbb{S}^2$, into (1) gives, at order δ , the linear equation

$$\partial_t \mathbf{n} = (\pm \mu - h)\mathbf{n} \times \hat{\mathbf{e}}_3 \pm \hat{\mathbf{e}}_3 \times (\alpha \partial_t \mathbf{n} - \partial_x^2 \mathbf{n} + \beta \mathbf{n} \times \hat{\mathbf{e}}_3),$$

which may be written in complex form as

$$\partial_t n \pm \beta n = i (\alpha \partial_t n - \partial_x^2 n - (h \mp \mu)n).$$

Its eigenvalue problem diagonalizes in Fourier space (for x) and yields the matrix eigenvalue problem

$$\begin{vmatrix} \pm\beta - \lambda & \Lambda \\ -\Lambda & \pm\beta - \lambda \end{vmatrix} = 0,$$

where $\Lambda = \pm\mu - h \mp \alpha\lambda \mp \ell^2$ with ℓ the Fourier wave number. The determinant reads

$$(\pm\beta - \lambda)^2 = -\Lambda^2 \quad \Leftrightarrow \quad \pm\beta - \lambda = \pm i\Lambda,$$

Considering real and imaginary parts this leads to

$$\begin{aligned} (1 + \alpha^2)\Re(\lambda) &= \pm\beta - \alpha(\ell^2 \pm h - \mu) = \alpha(\mu \mp (h - \beta/\alpha) - \ell^2) \\ \Im(\lambda) &= -\Re(\lambda) \pm \beta/\alpha, \end{aligned}$$

so that the maximal real part has $\ell = 0$.

Motivated by the rotation symmetry about the $\hat{\mathbf{e}}_3$ -axis, consider detuned coordinates, rotating about the m_3 -axis with frequency β/α . A straightforward calculation yields that Λ is modified to take the value $\Lambda \mp \beta/\alpha$ so that at criticality, the spectrum touches the origin in the complex plane at $\ell = \pm\beta/\alpha$. This is reminiscent of the spectral configuration of a Turing instability where, however, the spectrum near the origin lies on the real axis. In the present case, the spectrum extends along a complex conjugate pair of half lines with nonzero slope into the complex plane. It therefore seems natural that the modulation equation describing the dynamics near onset is the real Ginzburg-Landau equation (21), but we are not aware of its derivation and justification in the present context, and we do not pursue this here. Instead, we next discuss the existence and emergence of the expected spatio-temporal patterns: wavetrains and coherent structures. Indeed, the following existence and stability analyses for wavetrains are consistent with the ‘Eckhaus-scenario’ for wavetrains resulting from a Turing instability, though there are some differences.

The formulas for real- and imaginary parts immediately give the results mentioned in §1 and

Lemma 1 *The constant magnetizations $\mathbf{m} = \pm\hat{\mathbf{e}}_3$ are (strictly) L^2 -stable if and only if the anisotropy is subsubcritical ($-\mu > |h - \beta/\alpha|$), and both are unstable if and only if it is supercritical ($\mu > |h - \beta/\alpha|$). The instabilities are of Turing-type with wavenumber β/α .*

Remark 1 *The result extends to the more general situation of (5) with $|c| < 1$. In fact, linearization leads to the analogous equation*

$$\partial_t \mathbf{n} = (\pm\mu - h)\mathbf{n} \times \hat{\mathbf{e}}_3 \pm \hat{\mathbf{e}}_3 \times (\alpha \partial_t \mathbf{n} - \partial_x^2 \mathbf{n} + \beta^\pm \mathbf{n} \times \hat{\mathbf{e}}_3)$$

with $\beta^\pm = \beta/(1 \pm c)$ at $m_3 = \pm 1$, respectively.

4 Wavetrains

To exploit the rotation symmetry about the $\hat{\mathbf{e}}_3$ -axis, we change to polar coordinates in the planar components $m = (m_1, m_2)$ of the magnetization $\mathbf{m} = (m, m_3)$. With $m = r \exp(i\varphi)$ equation (1) changes to

$$\begin{pmatrix} \alpha & -1 \\ 1 & \alpha \end{pmatrix} \begin{pmatrix} r^2 \partial_t \varphi \\ \partial_t m_3 \end{pmatrix} = \begin{pmatrix} \partial_x(r^2 \partial_x \varphi) \\ \partial_x^2 m_3 + |\partial_x \mathbf{m}|^2 m_3 \end{pmatrix} + r^2 \begin{pmatrix} \beta \\ h - \mu m_3 \end{pmatrix}, \quad (14)$$

where

$$|\partial_x \mathbf{m}|^2 = (\partial_x r)^2 + r^2 (\partial_x \varphi)^2 + (\partial_x m_3)^2 \quad \text{and} \quad r^2 + m_3^2 = 1.$$

This can be seen as follows. In view of (3), with \mathbf{h}_{eff} replaced by the extended effective field $\mathbf{H}_{\text{eff}} = \mathbf{h}_{\text{eff}} - \mathbf{m} \times \mathbf{j}$ as is (9) and taking into account (11), (1) reads

$$\alpha \partial_t \mathbf{m} + \mathbf{m} \times \partial_t \mathbf{m} = \partial_x^2 \mathbf{m} + (h - \mu m_3) \hat{\mathbf{e}}_3 + (|\partial_x \mathbf{m}|^2 + \mu m_3^2 - h m_3) \mathbf{m} - \beta \mathbf{m} \times \hat{\mathbf{e}}_3.$$

The third component of the above equation is the second component of (14), whereas the first component of (14) is obtained upon inner multiplication by $\mathbf{m}^\perp = (m^\perp, 0) = (ie^{i\varphi}, 0)$ and taking into account that $\mathbf{m} \times \hat{\mathbf{e}}_3 = -\mathbf{m}^\perp$.

The rotation symmetry has turned into the shift symmetry $\varphi \mapsto \varphi + \text{const}$. In full spherical coordinates $\mathbf{m} = \begin{pmatrix} e^{i\varphi} \sin \theta \\ \cos \theta \end{pmatrix}$, (14) further simplifies to

$$\begin{pmatrix} \alpha & -1 \\ 1 & \alpha \end{pmatrix} \begin{pmatrix} \sin \theta \partial_t \varphi \\ -\partial_t \theta \end{pmatrix} = \begin{pmatrix} 2 \cos \theta \partial_x \theta \partial_x \varphi + \sin \theta \partial_x^2 \varphi \\ -\partial_x^2 \theta + \sin \theta \cos \theta (\partial_x \varphi)^2 \end{pmatrix} + \sin \theta \begin{pmatrix} \beta \\ h - \mu \cos \theta \end{pmatrix}. \quad (15)$$

4.1 Existence of wavetrains

Wavetrains are solutions of the form $\mathbf{m}(x, t) = \mathbf{m}_*(kx - \omega t)$, where k is referred to as the wavenumber and ω as the frequency. A natural type of wavetrains are relative equilibria with respect to the phase shift symmetry for which $\varphi = kx - \omega t$ and m_3, r are constant. See Figure 1 for an illustration.

Substituting this ansatz into (15) yields the algebraic equations

$$\begin{pmatrix} \alpha & -1 \\ 1 & \alpha \end{pmatrix} \begin{pmatrix} -\sin(\theta)\omega \\ 0 \end{pmatrix} = \begin{pmatrix} 0 \\ \sin(\theta) \cos(\theta) k^2 \end{pmatrix} + \sin(\theta) \begin{pmatrix} \beta \\ h - \mu \cos(\theta) \end{pmatrix}.$$

Thus either $\theta \equiv 0 \pmod{\pi}$ or

$$\begin{aligned} -\alpha\omega &= \beta \\ -\omega &= (k^2 - \mu)m_3 + h. \end{aligned}$$

In the first case we have $r = 0$, which corresponds to the constant upward or downward magnetizations, $(r, m_3) = (0, \pm 1)$ with unspecified k and ω .

In the second case, first notice that absence of dissipation ($\alpha = 0$) implies absence of magnetic field ($\beta = 0$) and there is a two-parameter set of wavetrains given by the second equation.

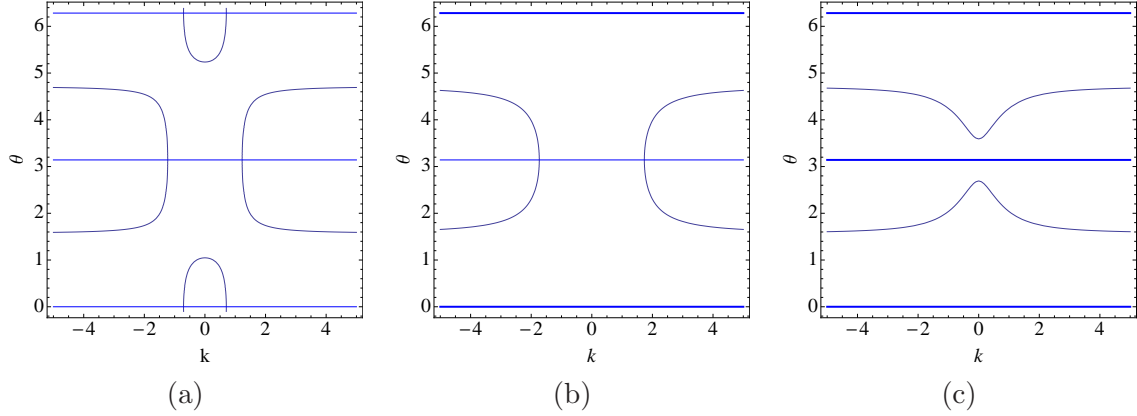


Figure 4: Plots of equilibrium locations in the (k, m_3) -plane including the trivial equilibria $\pm \hat{e}_3$ plotted with thick line if stable (when not intersecting wavetrain parameters). Compare Figure 5. See (17). (a) supercritical (easy plane) anisotropy ($\mu = 1$, $h - \beta/\alpha = 1/2$), (b) subcritical anisotropy ($\mu = 1$, $h - \beta/\alpha = 2$) no homogeneous oscillations ($k = 0$) exist, and (c) subsubcritical (easy axis) anisotropy $\mu = -1$, $h - \beta/\alpha = 0.9$.

The case we are interested in is $\alpha > 0$ and the existence conditions can be conveniently written as

$$\omega = -\frac{\beta}{\alpha} \quad (16)$$

$$\cos(\theta) = \frac{h - \beta/\alpha}{\mu - k^2}, \quad (\mu \neq k^2). \quad (17)$$

Here $\mu = k^2$ happens only in the easy plane case $\mu \geq 0$, and $\alpha h = \beta$ (with θ unspecified). Notably, all wavetrains oscillate with frequency given by the ratio of applied current and dissipation.

An involution symmetry involving parameters is

$$(h - \beta/\alpha, \theta) \rightarrow (\beta/\alpha - h, \theta + \pi), \quad (18)$$

so that the sign of $h - \beta/\alpha$ is irrelevant for the qualitative picture.

Solvability of (17) requires that $|\mu - k^2| > |h - \beta/\alpha|$ (unless $r = 0$), so that only for super- and subsubcritical anisotropy,

$$|\mu| > |h - \beta/\alpha|, \quad (19)$$

there are wavetrains with wavenumber in an interval around $k = 0$. In other words, non-trivial spatially nearly homogeneous oscillations require sufficiently small (in absolute value) difference between applied magnetic field and oscillation frequency (ratio of applied current and dissipation). The transition into this regime goes via the ‘Turing’ instability from §3. Combining (19) with Lemma 1 and straightforward analysis of (17) gives the following lemma. The three types of solution sets are plotted in Figure 4. Clearly, the solution sets are symmetric with respect to the signs of k and θ , respectively.

Theorem 1 *There are three types of wavetrain parameter sets solving (17):*

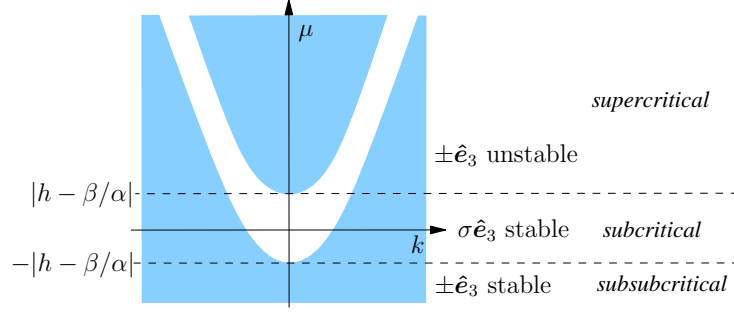


Figure 5: Sketch of existence region (shaded) in the (k, μ) -plane, with boundary given by (19) for $\sigma := \text{sgn}(h - \beta/\alpha) \neq 0$. The sign of σ determined which of $\pm \hat{e}_3$ is stable in th

1. For supercritical anisotropy there is one connected component of wavetrain parameters including $k = 0$, and two connected components with unbounded $|k|$, each with constant sign of k .
2. For subcritical anisotropy there are two connected components with unbounded $|k|$, each with constant sign of k .
3. For subsubcritical anisotropy there are two connected components, each a graph over the k -axis.

The Turing-type instabilities of $\pm \hat{e}_3$ noted in §3 at the transition from sub- to supercritical anisotropy is a supercritical bifurcation in the sense that solutions emerge at the loss of stability of the basic solution, here $\pm \hat{e}_3$, while that from sub- to subsubcritical is subcritical in the sense that solutions emerge at the gain of stability.

A fruitful viewpoint on existence conditions for wavetrains is to consider the frequency as a function of the wavenumber, which is referred to as the nonlinear dispersion relation. This is degenerate here, because the wavetrain frequency ω is independent of the wavenumber k in (16). As a consequence, the group velocity $d\omega/dk$, which describes the motion of perturbations by localized wave packets, equals the phase velocity ω/k for all wavetrains.

With the nonlinear dispersion relation in mind, it is customary to consider the existence region of wavetrains in wavenumber-parameter space. This is given by (17) and is periodic in θ , with $r = 0$ (zero amplitude) at $\theta \equiv 0 \pmod{\pi}$, which gives the boundary for nontrivial amplitude,

$$\mu = k^2 \pm (h - \beta/\alpha), \quad (20)$$

a pair quadratic parabolas in (k, μ) -space. The solution set in this projection is sketched in Figure 5. Remark that this set is non-empty for any parameter set $\alpha, \beta, h \in \mathbb{R}$ of (1). However, not all wavenumbers are possible due to the geometric constraint. Notably, the existence region consists of two disjoint sets, one contained in $\{\mu > 0\}$ with convex boundary and one extending into $\{\mu < 0\}$ with concave boundary. This again highlights the super- and subcritical nature of the wavetrain emergence noted in Theorem 1. From this, we would expect an exchange of stability, so that only in the supercritical case stable wavetrains emerge.

Before proving this, let us briefly discuss the origins of this expectation. The fact that frequencies are constant means that in co-rotating ('detuned') coordinates $\theta = \varphi - \frac{\beta}{\alpha}t$ the wavetrains have frequency zero and are thus stationary. The situation is then reminiscent of the (cubic) real Ginzburg-Landau equation mentioned in §3,

$$\partial_t A = \partial_x^2 A + \tilde{\mu} A \mp A|A|^2, \quad A(x, t) \in \mathbb{C}, \quad (21)$$

which describes the dynamics near pattern forming Turing instabilities and possesses the gauge-symmetry $A \rightarrow e^{i\varphi} A$. The solution $A = 0$ becomes unstable as $\tilde{\mu}$ becomes positive, which is the analogue of $\pm \hat{e}_3$ losing stability as μ crosses $\pm(h - \beta/\alpha)$.

Concerning wavetrains, the analogue of the symmetry group ansatz above is $A = r e^{kx - \omega t}$, $r \in \mathbb{R}$ the amplitude, which yields

$$\omega = 0, \quad \mu = k^2 \pm r^2.$$

In particular, all these wavetrains are stationary and the existence region, bounded by $r = 0$, is a parabola in (k, μ) -space, convex in the '+'-case and concave otherwise. A stability analysis of these wavetrains (which we omit) shows that only in the convex (supercritical) case stable wavetrains emerge, and these lie in the so-called Eckhaus region $\mu \geq 3k^2$. Hence, the aforementioned expectation, which is fully justified in the next section. The overall picture for (1) is thus *a combination of a supercritical ($\mu > 0$) and a subcritical ($\mu < 0$) Turing instability*, connected in parameter space via μ .

We have only considered the special case of (5) with $c = 0$, for otherwise (16) and (17) give rise to a quadratic equation for m_3 . For a parameter set away from special points, however, there exists for $0 < |c| \ll 1$ a unique solution m_3 which is compatible with the geometric constraint. In this generic situation the considerations on spectral stability to be carried out in Section 4.2 hold true by continuous differentiability.

4.2 Stability of wavetrains

In this section spectral stability of wavetrains is determined. For convenience, the comoving frame $y = x - c_{\text{ph}} t$ is considered with $c_{\text{ph}} = \omega/k$ the wavespeed. In this variable the wavetrain is an equilibrium of (14). Again for convenience, time is rescaled to $t = (1 + \alpha^2)\tau$. The explicit formulation of (14) then reads

$$\partial_\tau \begin{pmatrix} \varphi \\ m_3 \end{pmatrix} = \begin{pmatrix} \alpha(\partial_y(r^2 \partial_y \varphi)/r^2 + \beta) + (\partial_y^2 m_3 + |\partial_y \mathbf{m}|^2 m_3)/r^2 + h - \mu m_3 + c_{\text{ph}} \partial_y \varphi \\ \alpha(\partial_y^2 m_3 + |\partial_y \mathbf{m}|^2 m_3 + r^2(h - \mu m_3)) - \partial_y(r^2 \partial_y \varphi) - r^2 \beta + c_{\text{ph}} \partial_y m_3 \end{pmatrix}, \quad (22)$$

where $r^2 = 1 - m_3^2$.

Let $\mathcal{F} = (\mathcal{F}_1, \mathcal{F}_2)^t$ denote the right hand side of (22). Wavetrains have constant r and m_3 so that quadratic terms in their derivatives can be discarded for the linearization \mathcal{L} of \mathcal{F} in a

wavetrain, and from $|\partial_y \mathbf{m}|^2$ only $r^2(\partial_y \varphi)^2$ is relevant. The components of \mathcal{L} are

$$\begin{aligned}\partial_\varphi \mathcal{F}_1 &= \alpha \partial_y^2 + c_{\text{ph}} \partial_y + 2km_3 \partial_y \\ \partial_{m_3} \mathcal{F}_1 &= r^{-2} \partial_y^2 + k^2 - \mu - 2\alpha km_3 r^{-2} \partial_y \\ \partial_\varphi \mathcal{F}_2 &= 2\alpha km_3 r^2 \partial_y - r^2 \partial_y^2 \\ \partial_{m_3} \mathcal{F}_2 &= \alpha \partial_y^2 + \alpha r^2 (k^2 - \mu) + c_{\text{ph}} \partial_y - 2\alpha m_3 (m_3 k^2 + h - \mu m_3) + 2m_3 (k \partial_y + \beta) \\ &= \alpha \partial_y^2 + \alpha r^2 (k^2 - \mu) + c_{\text{ph}} \partial_y + 2m_3 k \partial_y,\end{aligned}$$

where the last equation is due to (17). Since all coefficients are constant, the eigenvalue problem

$$\mathcal{L}u = \lambda u$$

is solved by the characteristic equation arising from an exponential ansatz $u = \exp(\nu y)u_0$, which yields the matrix

$$A(\nu, c_{\text{ph}}) := \begin{pmatrix} \alpha \nu^2 + (c_{\text{ph}} + 2km_3)\nu & -r^{-2}\nu(-\nu + 2\alpha km_3) + k^2 - \mu \\ r^2\nu(-\nu + 2\alpha km_3) & \alpha \nu^2 + (c_{\text{ph}} + 2km_3)\nu + \alpha r^2(k^2 - \mu) \end{pmatrix}.$$

The characteristic equation then reads

$$\begin{aligned}d_{c_{\text{ph}}}(\lambda, \nu) &:= |A(\nu, c_{\text{ph}}) - \lambda| = |A(\nu, 0) - (\lambda - i\nu c_{\text{ph}})| = d_0(\lambda - c_{\text{ph}}\nu, \nu) \\ d_0(\lambda, \nu) &= \lambda^2 - \text{tr} A(\nu, 0)\lambda + \det A(\nu, 0)\end{aligned}\tag{23}$$

with trace and determinant of $A(\nu, 0)$

$$\begin{aligned}\text{tr} A(\nu, 0) &= 2\nu(\alpha \nu + 2km_3) + \alpha r^2(k^2 - \mu) \\ \det A(\nu, 0) &= (1 + \alpha^2)\nu^2(\nu^2 + 4k^2 m_3^2 + r^2(k^2 - \mu)) \\ &= (1 + \alpha^2)\nu^2 \left(\nu^2 + (3k^2 + \mu) \frac{(\beta/\alpha - h)^2}{(k^2 - \mu)^2} + k^2 - \mu \right).\end{aligned}$$

In the last equation (17) was used.

The characteristic equation is also referred to as the *complex dispersion relation*. The spectrum of \mathcal{L} , for instance in $L^2(\mathbb{R})$, consists of solutions for $\nu = i\ell$ and is purely essential spectrum (in the sense that $\lambda - \mathcal{L}$ is not a Fredholm operator with index zero). Indeed, setting $\nu = i\ell$ corresponds to Fourier transforming in y with Fouriermode ℓ . Note that the solution $d(0, 0) = 0$ stems from spatial translation symmetry in y .

The real part of solutions λ of (23) does not depend on c_{ph} , which means that spectral stability is independent of c_{ph} and is therefore completely determined by $d_0(\lambda, i\ell) = 0$.

First note the eigenvalues $A(0, 0)$ are 0 and $\alpha r^2(k^2 - \mu)$ so that *in the easy axis case* $\mu < 0$ *all wavetrains are unstable*. In the easy plane case $\mu > 0$ the wavetrains for $k^2 \leq \mu$ have a chance to be spectrally stable. In the following we therefore restrict to $\mu > 0$ and $k^2 < \mu$ and check the possible marginal stability configurations case by case.

Sideband instability. A sideband instability occurs when the curvature of the curve of essential spectrum attached to the origin changes sign so that the essential spectrum extends into positive real parts. Let $\tilde{\lambda}_0(\ell)$ denote the curve of spectrum of $A(i\ell, 0)$ attached to the origin, that is $\tilde{\lambda}_0(0) = 0$, and let $'$ denote the differentiation with respect to ℓ . Derivatives of $\tilde{\lambda}_0$ can be computed by implicit differentiation of

$$\det(A(i\ell, 0) - \lambda) = \det A(i\ell, 0) + \lambda^2 - \operatorname{tr}(A(i\ell, 0))\lambda = 0.$$

Since $\partial_\nu \det A(0, 0) = 0$ we have $\tilde{\lambda}'_0(0) = 0$ and therefore

$$\tilde{\lambda}''_0(0) = -\frac{\partial_\nu^2 \det A(0, 0)}{\operatorname{tr} A(0, 0)} = \frac{1 + \alpha^2}{\alpha r^2(\mu - k^2)} C,$$

where $D = (3k^2 + \mu) \frac{(\beta/\alpha - h)^2}{(k^2 - \mu)^2} + k^2 - \mu$.

At $k = 0$ (which means $\mu > \beta/\alpha - h$) we have $D = (\beta/\alpha - h)^2/\mu - \mu = (m_3^2 - 1)\mu < 0$ so that $\tilde{\lambda}''_0(0) < 0$, which implies stable sideband. Since $k^2 \neq \mu$, sideband instabilities are sign changes of

$$\begin{aligned} f(K) &:= (K - \mu)^2 D = (3K + \mu)(\beta/\alpha - h)^2 + (K - \mu)^3 \\ &= K^3 - 3\mu K^2 + 3(\mu^2 + (\beta/\alpha - h)^2)K + \mu(-\mu^2 + (\beta/\alpha - h)^2), \end{aligned}$$

where $K = k^2$.

For $\mu > 0$, f is monotone increasing for positive K : $f'(0) > 0$ and $f' \neq 0$ for real K by direct calculation. Since $f(0) < 0$ and $f(\mu) > 0$ (recall $\mu > \beta/\alpha - h$ for existence) there is precisely one real root to $f(k^2) = 0$ in $k^2 < \mu$. Therefore, for all $\mu > 0$ precisely one sideband instability occurs in $k^2 < \mu$ for increasing k^2 from zero. In Figure 6 we plot the resulting stability region.

For later purposes note that the non-zero solutions ν to

$$d_0(0, \nu) = \det A(\nu, 0) = (1 + \alpha^2)\nu^2(\nu^2 + D) = 0$$

change at the sideband instability $D = 0$ from positive and negative real to a complex conjugate pair.

Hopf instability. A Hopf instability occurs when the essential spectrum touches the imaginary axis at nonzero values, that is, there is $\gamma \neq 0$ so that $d_0(i\gamma, i\ell) = 0$. The imaginary part reads $(-2\alpha\ell^2 + \alpha r^2(k^2 - \mu))\gamma = 0$ and $\gamma \neq 0$ implies $2\ell^2 = r^2(k^2 - \mu)$. Hence, there is no Hopf instability in the range $k^2 < \mu$. Recall that wavetrains with $k^2 > \mu$ are already unstable.

Turing instability. A Turing instability occurs when the spectrum touches the origin for nonzero ℓ , that is, there is $\ell \neq 0$ so that $d_0(0, i\ell) = 0$, which means $\det A(i\ell, 0) = 0$. Touching the origin means in addition $\partial_\ell \det A(i\ell) = 0$. However, $\det A(i\ell, 0) = (1 + \alpha^2)\ell^2(\ell^2 - D)$ for $D \neq 0$ away from sideband instabilities. Since $\ell^2 = D > 0$ implies unstable sideband there are no relevant solutions.

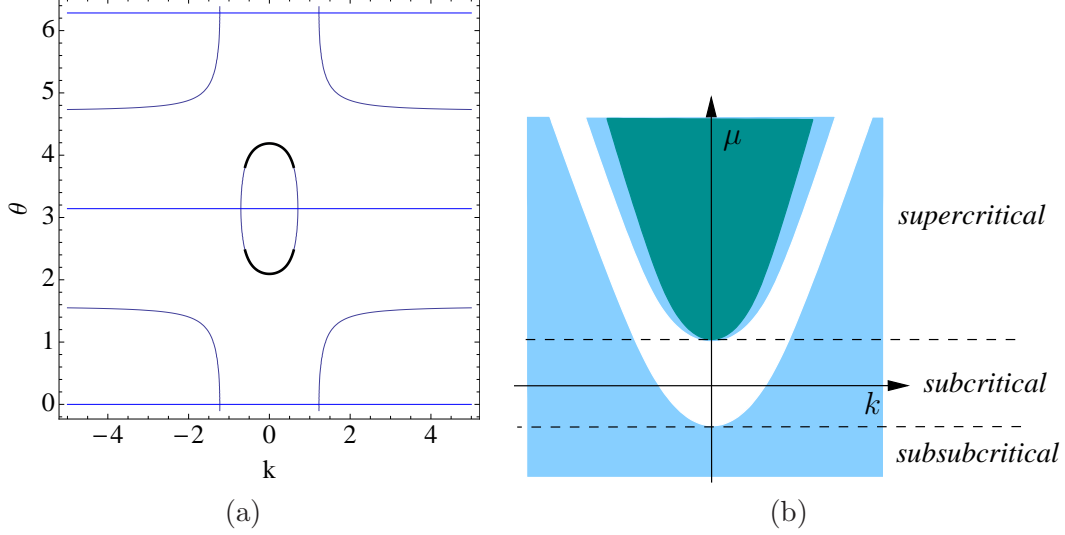


Figure 6: Analogues of Figures 4(a) and 5 with stable range of wavetrains in (a) bold line, and in (b) the dark shaded region.

Fold. A fold means that a curve of spectrum crosses the origin upon parameter variation. However, the sideband calculation shows that there is always a unique curve of spectrum attached to the origin for $k^2 \neq \mu$, which holds except at $h = \beta/\alpha$.

This exhausts the list of possible marginally stable spectral configuration and we conclude that, in analogy to the real Ginzburg-Landau equation, only sideband instabilities occur.

Taking into account that $k^2 = \mu$ for a wavetrain can occur only if $h = \alpha/\beta$ we thus have

Theorem 2 *All wavetrains whose wavenumber k satisfies $k^2 > \mu$ are unstable. For $\mu > 0$ there is $k_* > 0$ such that wavetrains with wavenumber $|k| < k_*$ are spectrally stable, while those with $|k| > k_*$ are unstable. In case $h \neq \alpha/\beta$ a sideband instability occurs at $k = \pm k_*$. There is no secondary instability for $k^2 < \mu$. Nontrivial spectrally stable wavetrains exist only for supercritical anisotropy, $|h - \beta/\alpha| < \mu$.*

5 Coherent structures

The coexistence of wavetrains and constant magnetizations raises the question how these interact. In this section we study solutions that spatially connect wavetrains in a coherent way. In order to locate such solutions induced by symmetry we make the ansatz

$$\begin{aligned}\xi &= x - st \\ \varphi &= \phi(\xi) + \Omega t \\ \theta &= \theta(\xi),\end{aligned}\tag{24}$$

with constant s, Ω . Solutions of (14) of this form are generalized travelling waves to (1) with speed s that have a superimposed oscillation about \hat{e}_3 with frequency Ω .

Substituting ansatz (24) into (15) with $' = d/d\xi$ and $q = \phi'$ gives, after division by $\sin(\theta)$, the ODEs

$$\begin{pmatrix} \alpha & -1 \\ 1 & \alpha \end{pmatrix} \begin{pmatrix} \sin(\theta)(\Omega - sq) \\ -s\theta' \end{pmatrix} = \begin{pmatrix} 2\cos(\theta)\theta'q + \sin(\theta)q' \\ -\theta'' + \sin(\theta)\cos(\theta)q^2 \end{pmatrix} + \sin(\theta) \begin{pmatrix} \beta \\ h - \mu\cos(\theta) \end{pmatrix}, \quad (25)$$

on the cylinder $(\theta, q) \in S^1 \times \mathbb{R}$, which is the same as $\{(m_3, r, q) \in \mathbb{R}^3 : m_3^2 + r^2 = 1\}$.

Wavetrains. Steady states with vanishing ξ -derivative correspond to the wavetrains discussed in §4 which have constant wavenumber $k = q = d\phi/d\xi$, frequency $\omega = sq - \Omega$ and amplitude r in m -space. Notably, for $s \neq 0$, steady states of (25) have the selected wavenumber q given by

$$q = \frac{\Omega - \beta/\alpha}{s}. \quad (26)$$

The θ -value of steady states solves $\sin(\theta) = 0$, i.e., $r = 0$, or $\cos(\theta)(q^2 - \mu) + h - \beta/\alpha = 0$, where the latter is the same as the wavetrain existence condition (17) with k replaced by q . In other words, the ansatz (24) for $s \neq 0$ removes all equilibria with wavenumber $k \neq \frac{\Omega - \beta/\alpha}{s}$.

Coherent structure ODEs. Writing (25) as an explicit ODE gives

$$\begin{aligned} \theta' &= p \\ p' &= \sin(\theta) (h + (q^2 - \mu)\cos(\theta) - (\Omega - sq)) + \alpha sp \\ q' &= \alpha(\Omega - sq) - \beta + \frac{s - 2\cos(\theta)q}{\sin(\theta)}p, \end{aligned} \quad (27)$$

whose study is the subject of the following sections. For later use we also note the ‘desingularization’ by the (singular) coordinate change $p = \sin(\theta)\tilde{p}$ so that $\tilde{p}' = p'/\sin(\theta) - \tilde{p}^2\cos(\theta)$, which gives

$$\begin{aligned} \theta' &= \sin(\theta)\tilde{p} \\ \tilde{p}' &= h + (q^2 - \mu)\cos(\theta) - (\Omega - sq) + \alpha s\tilde{p} - \cos(\theta)\tilde{p}^2 \\ q' &= \alpha(\Omega - sq) - \beta + (s - 2\cos(\theta)q)\tilde{p}. \end{aligned} \quad (28)$$

Hence, (27) is equivalent to (28) except at zeros of $\sin(\theta)$. In particular, for $\tilde{p} = 0$ the equilibria of (28) are those of (27), but $\theta = n\pi$, $n \in \mathbb{Z}$ are invariant subspaces which may contain equilibria with $\tilde{p} \neq 0$.

5.1 Stationary coherent structures ($s = 0$)

In this section we consider the case $s = 0$ (which does not imply time-independence), where equations (27) reduce to

$$\begin{aligned} \theta'' &= \sin(\theta) (h - \Omega + (q^2 - \mu)\cos(\theta)) \\ q' &= \alpha\Omega - \beta - 2\cot(\theta)\theta'q, \end{aligned} \quad (29)$$

where $\cot(\theta) = \frac{\cos(\theta)}{\sin(\theta)}$.

In case $\Omega \neq \alpha/\beta$ there are no equilibria and it will be shown at the end of this section that there are no coherent structure-type solutions in that case. For $\Omega = \alpha/\beta$, system (29) is invariant under the reflection $q \rightarrow -q$ so that $\{q = 0\}$ is an invariant plane which separates the three dimensional phase space. In particular, *there cannot be connections between equilibria (=wavetrains) with opposite signs of q , that is, sign reversed spatial wavenumbers.*

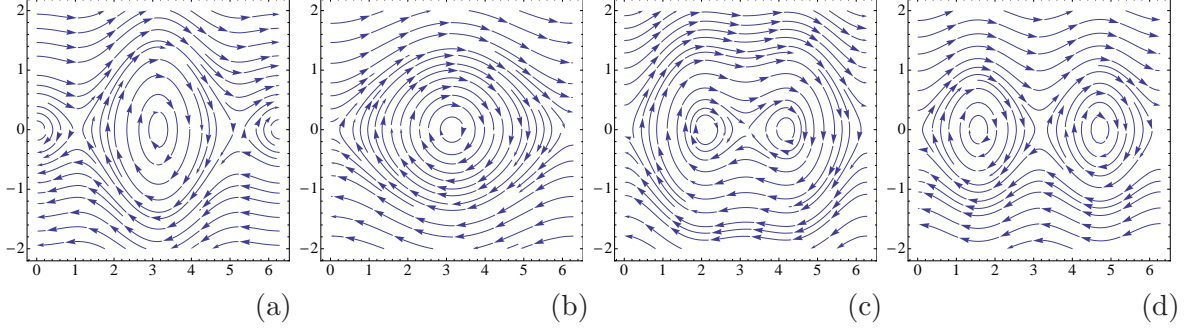


Figure 7: Phase plane streamplots of (30) with MATHEMATICA (θ horizontal, θ' vertical axes). (a)-(c) have $h - \Omega = 1/2$. (a) supercritical anisotropy ($\mu = 1$), (b) subcritical ($\mu = 0$), (c) subsubcritical ($\mu = -1$), (d) degenerate subsubcritical case $h = \Omega$, $\mu = -1$.

5.1.1 Homogeneous solutions ($q = 0$)

Solutions in the invariant set $\{q = 0\}$ have the form $m(\xi) = r(\xi) \exp(it\Omega)$ and (25) turns into a second order ODE on the circle $\{m_3^2 + r^2 = 1\}$. The ODE for θ from (29) is given by the nonlinear pendulum equation

$$\theta'' = \sin(\theta) (h - \Omega - \mu \cos(\theta)), \quad (30)$$

which is invariant under $\theta \rightarrow -\theta$ and is Hamiltonian with potential energy

$$P_0(\theta) = \cos(\theta) (h - \Omega - \frac{\mu}{2} \cos(\theta)).$$

The symmetry (18) applies and we therefore assume in the following that $\Omega = \beta/\alpha < h$.

We plot the qualitatively different vector fields of (30) in Figure 7 and some profiles in Figure 3. Coherent structure solutions are completely characterized as in the figures, which we formulate next explicitly for the original PDE with $\mathbf{m} = (m, m_3)$, $m = r e^{i\varphi}$, $r = \sin(\theta)$, $m_3 = \cos(\theta)$. Homoclinic profiles may be interpreted as (dissipative) solitons. The heteroclinic connections in item 2(a) can be viewed as (dissipative) solitons with ‘phase slip’.

Theorem 3 *Let $s = 0$ and $\Omega = \alpha/\beta$ and consider solutions to (14) of the form (24) with φ constant in ξ , i.e., $q = 0$. These oscillate in time pointwise about the $\hat{\mathbf{e}}_3$ -axis with frequency $\Omega = \beta/\alpha$. Assume without loss of generality, due to (18), that $h > \Omega$.*

1. *Consider subcritical anisotropy $h - \Omega > |\mu| > 0$. There exist no nontrivial wavetrains with $q = 0$, and the coherent structure solutions with $q = 0$ are a pair of homoclinic profiles to $\hat{\mathbf{e}}_3$, and three one-parameter families of periodic profiles, one bounded and two semi-unbounded. The homoclinic profiles each cross once through $-\hat{\mathbf{e}}_3$ in opposite θ -directions. The limit points of the bounded curve of periodic profiles are $-\hat{\mathbf{e}}_3$ and the union of homoclinic profiles. Each of the homoclinics is the limit point of one of the semi-unbounded families, each of which has unbounded θ -derivatives. The profiles from the bounded family each cross $-\hat{\mathbf{e}}_3$ once during a half-period, the profiles of the unbounded family cross both $\pm \hat{\mathbf{e}}_3$ during one half-period.*

2. Suppose super- or subsubcritical anisotropy $|\mu| > h - \Omega$. There exists a wavetrain with $k = 0$, which is stable in the supercritical case ($\mu > 0$) and unstable in the subsubcritical case ($\mu < 0$). In (30) this appears in the form of two equilibria being the symmetric pair of intersection points of the wavetrain orbit and a meridian on the sphere, phase shifted by π in φ -direction. Details of the following can be read off Figure 7 analogous to item 1.
 - (a) In the supercritical case ($\mu > h - \Omega$) the coherent structure solutions with $q = 0$ are two pairs of heteroclinic connections between the wavetrain and its phase shift, and four curves of periodic profiles; two bounded and two semi-unbounded.
 - (b) In the subsubcritical case ($\mu < h - \Omega$) the coherent structure solutions with $q = 0$ are two pairs of homoclinic connections to $\pm \hat{e}_3$, respectively, and five curves of periodic profiles, three bounded and two semi-unbounded.
3. The degenerate case $h = \Omega$, $\mu < 0$ is the only possibility for profiles of stationary coherent structures to connect between $\pm \hat{e}_3$, which then come in a pair as in the corresponding panel of Figure 7. The remaining coherent structures with $q = 0$ are analogous to the supercritical case with $\pm \hat{e}_3$ and the pair of wavetrain and its phase shift interchanged.

Proof. As for wavetrains discussed in §4, the condition $\cos(\theta) = (h - \Omega)/\mu$ yields the existence criterion $|h - \Omega| < |\mu|$ for an equilibrium to (30) in $(0, \pi)$. The derivative of the right hand side of (30) at $\theta = 0$ is $h - \Omega - \mu$, which dictates the type of all equilibria and only saddles generate heteroclinic or homoclinic solutions.

It remains to study the connectivity of stable and unstable manifolds of saddles, which is given by the difference in potential energy $P_0(\theta)$. Since $P_0(0) - P_0(\pi) = 2(h - \Omega)$ the claims follow. ■

5.1.2 Non-homogeneous solutions ($q \neq 0$)

In order to study (29) for $q \neq 0$, we note the following first integral. Since $\Omega = \beta/\alpha$, the equation for q can be written as

$$(\log |q|)' = -2(\log |\sin(\theta)|)',$$

and therefore explicitly integrated. With integration constant $C = \sin(\theta(0))^2 |q(0)|$ this gives

$$q = \frac{C}{\sin(\theta)^2}. \quad (31)$$

Substituting this into the equation for θ yields the nonlinear pendulum

$$\theta'' = \sin(\theta) (h - \Omega - \mu \cos(\theta)) + C^2 \frac{\cos(\theta)}{\sin(\theta)^3}, \quad (32)$$

with singular potential energy

$$P(\theta) = P_0(\theta) + \frac{1}{2}C^2 \cot(\theta)^2.$$

The energy introduces barriers at multiples of π so that solutions for $q \neq 0$ cannot pass $\pm \hat{e}_3$, and as C increases the energy landscape becomes qualitatively independent of Ω, h, μ .

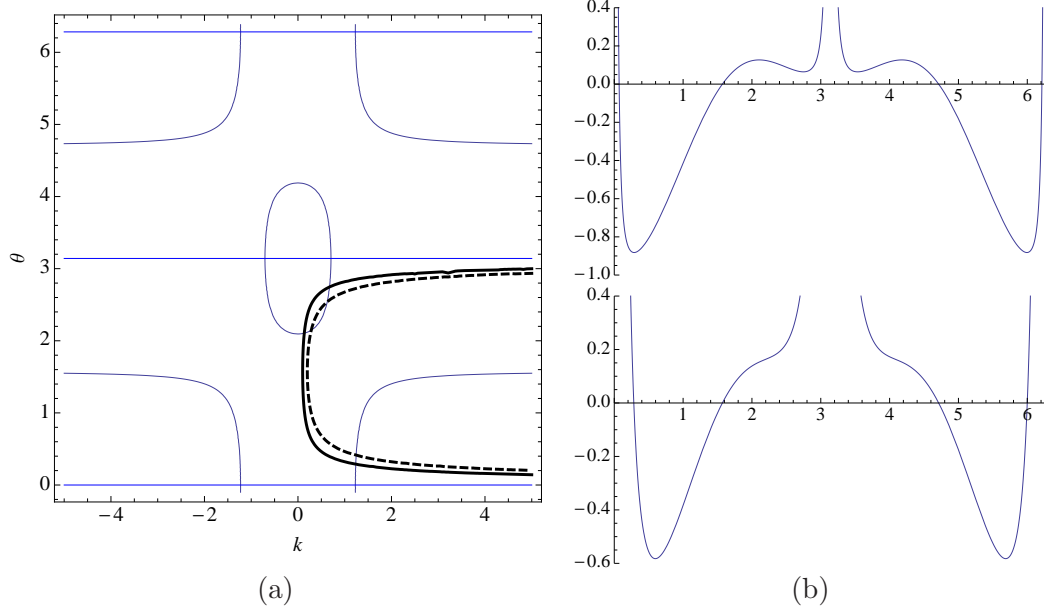


Figure 8: (a) Figure 6(a) with solutions to (31) for $\theta \in (0, \pi)$ and $C = 0.1$ (thick solid line), and $C = 0.4$ (thick dashed line). (b) Upper panel: potential $P(\theta)$ for parameters as in (a) and $C = 0.1$. Lower panel: same with $C = 0.4$.

As an immediate consequence of the energy barriers and the fact that only stable wavetrains are saddle points we get

Theorem 4 *Let $s = 0$ and $\Omega = \alpha/\beta$. Consider solutions to (14) of the form (24). Intersections in (q, θ) -space of the curve \mathcal{C} given by (31) with the wavetrain existence curves \mathcal{W} from (17) (with k replaced by q) are in one-to-one correspondence with equilibria of (29).*

Consider supercritical anisotropy $0 \leq h - \Omega < \mu$ and assume C is such that \mathcal{C} transversely intersects the component of \mathcal{W} which intersects $\{q = 0\}$. Then the intersection point with smaller q -value corresponds to a spectrally stable wavetrain, and in (29) there is a pair of homoclinic solutions to this wavetrain. All other intersection points are unstable wavetrains.

All other non-equilibrium solutions of the form (24) with $s = 0$ are periodic in ξ , and this is also the case for all other parameter settings.

The homoclinic orbit is a soliton-type solution to (1) with asymptotic state a wavetrain. See Figure 2 for a nearby solution with periodic (reduced) profile.

Notably, the tangential intersection of \mathcal{C} and \mathcal{W} is at the sideband instability.

In Figure 8 we plot an illustration in case of supercritical anisotropy $\mu > \Omega - h > 0$. In the upper panel of (b) the local maxima each generate a pair of homoclinic solutions to the stable wavetrain it represents. The values of q that it visits lie on the bold curve in (a), whose intersections with the curve of equilibria are the local maxima and minima. The lower panel in (b) has $C = 0.4$ and the local maxima disappeared. All solutions are periodic and lie on the thick dashed curve in (a).

5.1.3 Absence of wavetrains ($\Omega \neq \alpha/\beta$)

In this case the first integral $Q = \log(|q| \sin(\theta)^2)$ is monotone,

$$Q' = \frac{\Omega - \alpha/\beta}{q} \neq 0,$$

and therefore $|q|$ is unbounded as $\xi \rightarrow \infty$ or $\xi \rightarrow -\infty$. In view of (32), we also infer that θ oscillates so that there are no relevant solutions of the form (24).

5.2 Moving coherent structures

Using the desingularized system (28), we prove existence of some non-stationary coherent structures.

5.2.1 Fast front-type coherent structures ($|s| \gg 1$)

In this section we prove existence of fast front-type coherent structures with at least one asymptotic state of the profile being the constant up- or down-magnetization $\pm \hat{e}_3$.

As a first step, it is convenient to consider such solutions in the desingularized system (28).

Theorem 5 *For any bounded set of $(\alpha, \beta, \mu, \Omega_0, \Omega_1)$ there exists $s_0 > 0$ and neighborhood U of $M_0 := \{\theta \in [0, \pi], \tilde{p} = q - \Omega_1 = 0\}$ such that for all $|s| \geq s_0$ the following holds for (28) with $\Omega = \Omega_0 + \Omega_1 s$. There exists a pair of heteroclinic trajectories $(\theta_{\pm h}, \tilde{p}_{\pm h}, q_{\pm h})(\xi)$ in U with $\frac{d}{d\xi} \theta_h(\xi) = O(s^{-1})$, and $\lim_{\xi \rightarrow -\infty} \theta_{-h}(\tau \xi) = 0$, $\lim_{\xi \rightarrow \infty} \theta_{+h}(\tau \xi) = \pi$, where $\tau = \text{sgn}(s(h - \beta/\alpha - \mu))$.*

The local wavenumbers are always nontrivial, $q_{\pm h} \neq 0$, and the heteroclinics form a smooth family in s^{-1} with

$$\lim_{|\xi| \rightarrow \infty} q_{\pm h}(\xi) = \frac{1}{s} \left(\frac{h + \alpha\beta \mp \mu}{1 + \alpha^2} - \Omega \right) + O(s^{-2}).$$

On the spatial scale $\eta = \xi/s$ the heteroclinics solve, to leading order in s^{-1} , the ODE

$$\frac{d}{d\eta} \theta = \frac{\alpha}{1 + \alpha^2} \sin(\theta) \left(h - \frac{\beta}{\alpha} + (\Omega_1^2 - \mu) \cos(\theta) \right). \quad (33)$$

Before the proof we note the consequences of this for coherent structures in (27).

Corollary 1 *The heteroclinic solutions of Theorem 5 are in one-to-one correspondence with heteroclinic solutions to (27) that lie in U and connect $\theta = 0, \pi$ and/or the possible equilibrium at $\theta_1 := \arccos((h - \beta/\alpha)/\mu)$. For $\theta \in (0, \pi)$ all properties carry over to (27) with the bijection given by $p = \sin(\theta)\tilde{p}$.*

Some remarks are in order.

- The ODE (33) is the spatial variant of the temporal heteroclinic connection in (15): setting all space derivatives to zero, the θ -equation of (15) reads

$$-\partial_t \theta = \frac{\alpha}{1 + \alpha^2} \sin(\theta) \left(h - \frac{\beta}{\alpha} - \mu \cos(\theta) \right),$$

which is (33) with μ replaced by $\Omega_1^2 - \mu$ and up to possible direction reversal. Since $\Omega_1 = q$ on the slow manifold (i.e. at leading order), the reduced flow equilibria reproduce the wavetrain existence condition (17). This kind of relation between temporal dynamics and fast travelling waves formally holds for any evolution equation in one space dimension.

- For increasing speeds these solutions are decreasingly localized, hence far from a sharp transition. For $\Omega_1 \neq 0$ the azimuthal frequency increases with s .
- The uniqueness statement is limited, since in the (θ, p, q) -coordinates the neighborhood U from the theorem is ‘pinched’ near $\theta = 0, \pi$: a uniform neighborhood in (θ, \tilde{p}) has a sinus boundary in (θ, p) .

Concerning stability, we infer from Lemma 1 and Theorem 2 that none of these fronts can be stable in an L^2 -sense: always one of the asymptotic states is unstable. In the supercritical case $\pm \hat{e}_3$ are unstable, in the subcritical case one of $\pm \hat{e}_3$ is unstable and in the subsubcritical case the wavetrain with $\theta = \theta_1 \in (0, \pi)$ is unstable. However, it is not ruled out that these fronts are stable in a suitable weighted sense as invasion fronts into an unstable state, which we do not pursue further in this paper.

Proof (Theorem 5) Let us set $s = \varepsilon^{-1}$ so that the limit to consider is $\varepsilon \rightarrow 0$. Since we will rescale space with ε and ε^{-1} this means sign changes of s reflect the directionality of solutions.

The existence proof relies on a geometric singular perturbation argument and we shall use the terminology from this theory, see [8, 14], and also sometimes suppress the ε -dependence of θ, \tilde{p}, q .

Upon multiplying the \tilde{p} - and q -equations of (28) by ε we obtain the, for $\varepsilon \neq 0$ equivalent, ‘slow’ system

$$\begin{aligned}\theta' &= \sin(\theta)\tilde{p} \\ \varepsilon \tilde{p}' &= \alpha \tilde{p} + q - \Omega_1 + \varepsilon(h + (q^2 - \mu)\cos(\theta) - \Omega_0 - \cos(\theta)\tilde{p}^2) \\ \varepsilon q' &= \tilde{p} - \alpha(q - \Omega_1) + \varepsilon(\alpha\Omega_0 - \beta - 2\cos(\theta)q\tilde{p}).\end{aligned}\tag{34}$$

Setting $\varepsilon = 0$ gives the algebraic equations

$$A \begin{pmatrix} \tilde{p} \\ q \end{pmatrix} = -\Omega_1 \begin{pmatrix} -1 \\ \alpha \end{pmatrix}, \quad A = \begin{pmatrix} \alpha & 1 \\ 1 & -\alpha \end{pmatrix}.$$

Since $\det A = -(1 + \alpha^2) < 0$ the unique solution is $\tilde{p} = q - \Omega_1 = 0$ and thus the ‘slow manifold’ is M_0 as defined in the theorem, with ‘slow flow’ given by

$$\theta' = \sin(\theta)\tilde{p}.$$

Since $\tilde{p} = 0$ at $\varepsilon = 0$, M_0 is a manifold (a curve) of equilibria at $\varepsilon = 0$, so that the slow flow is in fact ‘superslow’ and will be considered explicitly below. Since the slow manifold is one-dimensional (and persists for $\varepsilon > 0$ as shown below) it suffices to consider equilibria for $\varepsilon > 0$. These lie on the one hand at $\theta = \theta_0 \in \{0, \pi\}$, if

$$A \begin{pmatrix} \tilde{p} \\ q \end{pmatrix} + \Omega_1 \begin{pmatrix} -1 \\ \alpha \end{pmatrix} + \varepsilon F(\tilde{p}, q) = 0, \quad F(\tilde{p}, q) := \begin{pmatrix} h + \sigma(q^2 - \mu) - \Omega_0 - \sigma\tilde{p}^2 \\ \alpha\Omega_0 - \beta - 2\sigma q\tilde{p} \end{pmatrix},$$

where $\sigma = \cos(\theta_0) \in \{-1, 1\}$. Since $\det A = -(1 + \alpha^2) < 0$ the implicit function theorem provides a locally unique curve of equilibria $(\tilde{p}_\varepsilon, q_\varepsilon)$ for sufficiently small ε , where

$$\left. \frac{d}{d\varepsilon} \right|_{\varepsilon=0} \begin{pmatrix} \tilde{p}_\varepsilon \\ q_\varepsilon \end{pmatrix} = -A^{-1}F(0,0) = -A^{-1} \begin{pmatrix} h - \sigma\mu - \Omega_0 \\ \alpha\Omega_0 - \beta \end{pmatrix}.$$

This proves the claimed location of asymptotic states.

On the other hand, for $\theta \neq 0$ system (28) is equivalent to (27). From the previous considerations of equilibria (=wavetrains) we infer that the unique equilibria in an ε -neighborhood of M_0 are those at $\theta = \theta_0$, $(\tilde{p}, q) = (\tilde{p}_\varepsilon, q_\varepsilon)$ together with the single solution θ_1 to (17), if it exists, with k replaced by $q = \varepsilon(\Omega_0 - \beta/\alpha)$.

Towards the persistence of M_0 as a perturbed invariant manifold for $|\varepsilon| > 0$, let us switch to the ‘fast’ system by rescaling the time-like variable to $\zeta = \xi/\varepsilon$. With $\dot{\theta} = d\theta/d\zeta$ etc., this gives

$$\begin{aligned} \dot{\theta} &= \varepsilon \sin(\theta) \tilde{p} \\ \dot{\tilde{p}} &= \alpha \tilde{p} + q - \Omega_1 + \varepsilon(h + (q^2 - \mu) \cos(\theta) - \Omega_0 - \cos(\theta) \tilde{p}^2) \\ \dot{q} &= \tilde{p} - \alpha(q - \Omega_1) + \varepsilon(\alpha\Omega_0 - \beta - 2\cos(\theta)q\tilde{p}). \end{aligned} \tag{35}$$

Note that M_0 is (also) a manifold of equilibria at $\varepsilon = 0$ in this system and the linearization of (35) in M_0 for transverse directions to M_0 is given by A . Since the eigenvalues of A , $\pm\sqrt{1+\alpha^2}$, are off the imaginary axis, M_0 is normally hyperbolic and therefore persists as an ε -close invariant one-dimensional manifold M_ε , smooth in ε and unique in a neighborhood of M_0 . See [8]. The aforementioned at least two and at most three equilibria lie in M_ε , and, M_ε being one-dimensional, these must be connected by heteroclinic orbits.

For the connectivity details it is convenient to derive an explicit expression of the leading order flow. We thus switch to the superslow time scale $\eta = \varepsilon\xi$ and set $\bar{p} = \tilde{p}/\varepsilon$, $\bar{q} = (q - \Omega_1)/\varepsilon$, which changes (34) to (subindex η means $d/d\eta$)

$$\begin{aligned} \theta_\eta &= \sin(\theta) \bar{p} \\ \varepsilon \bar{p}_\eta &= \alpha \bar{p} + \bar{q} + h + (\Omega_1^2 - \mu) \cos(\theta) - \Omega_0 + \varepsilon \cos(\theta) (\varepsilon(\bar{q}^2 - \bar{p}^2) + 2\bar{q}\Omega_1) \\ \varepsilon \bar{q}_\eta &= \bar{p} - \alpha \bar{q} + \alpha\Omega_0 - \beta - 2\varepsilon \cos(\theta) (\varepsilon \bar{q} \bar{p} + \Omega_1 \bar{p}). \end{aligned} \tag{36}$$

At $\varepsilon = 0$, solving the algebraic equations for \bar{p} provides the flow for θ given by

$$A^{-1} \begin{pmatrix} h + (\Omega_1^2 - \mu) \cos(\theta) - \Omega_0 \\ \alpha\Omega_0 - \beta \end{pmatrix} = \frac{1}{1 + \alpha^2} \begin{pmatrix} \alpha h - \alpha(\Omega_1^2 - \mu) \cos(\theta) - \beta \\ h - (\Omega_1^2 - \mu) \cos(\theta) - (1 + \alpha^2)\Omega_0 + \alpha\beta. \end{pmatrix}$$

so that the leading order superslow flow on the invariant manifold is given by (33). \blacksquare

Proof (Corollary 1) Recall that (28) and (27) are equivalent for $\theta \in (0, \pi)$. Next, we note that the limit of the vector field of (27) along such a heteroclinic from (28) is zero by construction. Hence, for each of the heteroclinic orbits in (28) of Theorem 5, there exist a heteroclinic orbit in (27) in the sense of the corollary statement. \blacksquare

5.2.2 Small amplitude moving coherent structures

In this section we consider all possible small amplitude coherent structures for speeds

$$s^2 > \frac{4q^2}{1 + \alpha^2}, \quad (37)$$

where $q \neq 0$ is an equilibrium q -value (26). Small amplitude means q must lie near a bifurcation point, which are the intersection points of the solution curves from (17) with $\theta = \theta_0 = 0, \pi$. This gives

$$\cos(\theta_0) (q^2 - \mu) = \frac{\beta}{\alpha} - h \quad (38)$$

and is only possible for super- and subcritical anisotropy.

We show that such coherent structures must be of front-type. Recall that for $s = 0$ there are also coherent structures with periodic and homoclinic (soliton-type) profiles. In the previous section we found front-type solutions when $h - \beta/\alpha$ enters $(-\mu, \mu)$, that is, the anisotropy changes from subcritical to super- or subsubcritical, and when the speed s is above a theoretical threshold. In this section, we give an explicit bound for this threshold in the small amplitude limit. We shall prove that for speeds satisfying (37), these points are pitchfork-type bifurcations in (28), which give rise to front-type coherent structures. As in the previous section, we locate such solutions in (27) from an analysis of (28). Remark that in the PDE (1) the pitchfork-type bifurcation corresponds to a Hopf-type bifurcation due to the superimposed oscillation about the \hat{e}_3 -axis.

Theorem 6 *Let $S_\varepsilon = (\alpha_\varepsilon, \beta_\varepsilon, h_\varepsilon, \mu_\varepsilon, \Omega_\varepsilon, s_\varepsilon)$ be a curve in the parameter space of (28) with $\varepsilon \in (-\varepsilon_0, \varepsilon_0)$ for some $\varepsilon_0 > 0$ sufficiently small such that $\alpha_\varepsilon > 0$ and $q_\varepsilon, S(\varepsilon)$ solve (26), (38) with q_ε strictly monotone increasing in ε , and at $\varepsilon = 0$.*

Then (28) with parameters S_ε has equilibria at $(\theta, \tilde{p}, q) = (\theta_0, 0, q_\varepsilon)$ and at $\varepsilon = 0$ the following occur.

1. *There is a pitchfork-type bifurcation in case $q_0 \neq \mu_0$ and $\theta_0 = 0$ or π : If $q_0 > \mu_0$ ($q_0 < \mu_0$) two equilibria bifurcate as ε changes from negative to positive (positive to negative), which are connected to $(\theta_0, 0, q_\varepsilon)$ by a heteroclinic connection, respectively. These are unique in a neighborhood U of $(\theta_0, 0, q_0)$.*

The heteroclinics converge to $(\theta_0, 0, q_\varepsilon)$ as $\text{sgn}(s(q^2 - \mu))\xi \rightarrow \infty$ so that a bifurcation in $\{q^2 < \mu\}$ is supercritical and subcritical in $\{q^2 > \mu\}$.

These bifurcations are not generic in the coordinates of (28), because its linearization in equilibria with $\theta = 0$ or π always has a kernel.

2. *There is no local bifurcation in case $q_0 - \mu_0 = h_0 - \beta_0/\alpha_0 = 0$ and $\theta_0 = \pi/2$: for $\varepsilon \neq 0$ there is at most one equilibrium and there are no small amplitude solutions to (27) in its vicinity.*

Analogous to Corollary 1 we have

Corollary 2 *The heteroclinic solutions of Theorem 6 are in one-to-one correspondence with heteroclinic solutions to (27), connecting to $\theta = 0$ or $\theta = \pi$ in U . Bounded solutions for $\theta \notin \{0, \pi\}$ are also in one-to-one correspondence.*

Proof (Theorem 6) The existence analysis of equilibria already implies the emergence of two symmetric equilibria under the stated conditions in item (1), and that there is at most one in item (2). Hence, it remains to show that the center manifold associated to the bifurcation is one-dimensional and to obtain the directionality of heteroclinics.

For the former it suffices to show that the linearization at the bifurcation point has only a simple eigenvalue on the imaginary axis, namely at zero. The linearization of (28) in any point with $\tilde{p} = 0$ (in particular for all relevant equilibria) gives the 3×3 matrix

$$\tilde{A} = \left(\begin{array}{c|cc} 0 & \sin(\theta) & 0 \\ \hline (\mu - q^2) \sin(\theta) & & \\ 0 & B & \end{array} \right), \quad B = \begin{pmatrix} \alpha s & 2q \cos(\theta) - s \\ s - 2q \cos(\theta) & \alpha s \end{pmatrix}.$$

In particular, for $\theta = \theta_0 = 0, \pi$ and for $\mu_0 = q_0^2$, the matrix \tilde{A} has a kernel with eigenvector $(1, 0, 0)^t$. The remaining eigenvalues are those of B . Since B has vanishing trace, its eigenvalues are either a complex conjugate pair (for $\det B > 0$) or a pair of sign reversed real numbers (for $\det B < 0$) or a double zero ($\det B = 0$). Since $\det B = 4q^2 \cos(\theta_0)^2 - (1 + \alpha^2)s^2$ the constraints in the theorem statement imply a simple zero eigenvalue and no further eigenvalues on the imaginary axis.

The simple eigenvalue on the imaginary axis implies existence of a one-dimensional center manifold that includes all equilibria near $(\theta_0, 0, q_0)$ for nearby parameters.

In case (1) the uniqueness of bifurcating equilibria on either side of the symmetry axes and invariance of the one-dimensional center manifold implies presence and local uniqueness of the claimed heteroclinic connections. In order to determine the directionality of these, we compute the leading order correction to the eigenvalues of \tilde{A} for $\theta = \theta_0 + \delta$. The straightforward calculation yields the eigenvalue of the bifurcation branch as

$$\frac{\alpha}{(1 + \alpha^2)s} (q^2 - \mu) \delta^2 + \mathcal{O}(\delta^4),$$

which gives the claimed directionality. ■

References

- [1] BERGER, L. Emission of spin waves by a magnetic multilayer traversed by a current. *Phys. Rev. B* 54, 13 (Oct. 1996), 9353–9358.
- [2] BERKOV, D., AND MILTAT, J. Spin-torque driven magnetization dynamics: Micromagnetic modeling. *J. Magn. Magn. Mat.* 320, 7 (April 2008), 1238–1259.
- [3] BERTOTTI, G. Spin-transfer-driven magnetization dynamics.
- [4] BERTOTTI, G., BONIN, R., D’AQUINO, M., SERPICO, C., AND MAYERGOYZ, I. Spin-wave instabilities in spin-transfer-driven magnetization dynamics. *IEEE Magnetics letters* 1 (2010), 3000104.
- [5] BERTOTTI, G., SERPICO, C., MAYERGOYZ, I. D., MAGNI, A., D’AQUINO, M., AND BONIN, R. Magnetization switching and microwave oscillations in nanomagnets driven by spin-polarized currents. *Phys. Rev. Lett.* 94 (Apr 2005), 127206.

- [6] CAPELLA, A., MELCHER, C., AND OTTO, F. Wave-type dynamics in ferromagnetic thin films and the motion of Néel walls. *Nonlinearity* 20, 11 (2007), 2519–2537.
- [7] CARBOU, G. Stability of static walls for a three-dimensional model of ferromagnetic material. *J. Math. Pures Appl. (9)* 93, 2 (2010), 183–203.
- [8] FENICHEL, N. Geometric singular perturbation theory for ordinary differential equations. *J. Differ. Equations* 31 (1979), 53–98.
- [9] GILBERT, T. A phenomenological theory of damping in ferromagnetic materials. *Magnetics, IEEE Transactions on* 40, 6 (nov. 2004), 3443 – 3449.
- [10] HASIMOTO, H. A soliton on a vortex filament. *J. Fluid Mech* 51, 3 (1972), 477–485.
- [11] HOEFER, M., ABLOWITZ, M., ILAN, B., PUFALL, M., AND SILVA, T. Theory of magnetodynamics induced by spin torque in perpendicularly magnetized thin films. *Physical review letters* 95, 26 (2005), 267206.
- [12] HOEFER, M., SOMMACAL, M., AND SILVA, T. Propagation and control of nanoscale magnetic-droplet solitons. *Phys. Rev. B.* 85 (2012), 214433.
- [13] HUBERT, A., AND SCHÄFER, R. *Magnetic Domains: The Analysis of Magnetic Microstructures*. Springer, August 1998.
- [14] JONES, C. K. Geometric singular perturbation theory. Johnson, Russell (ed.), Dynamical systems. Lectures given at the 2nd session of the Centro Internazionale Matematico Estivo (CIME) held in Montecatini Terme, Italy, June 13-22, 1994. Berlin: Springer-Verlag. Lect. Notes Math. 1609, 44-118 (1995)., 1995.
- [15] KRAVCHUK, V. P., VOLKOV, O. M., SHEKA, D. D., AND GAIDIDEI, Y. Periodic magnetization structures generated by transverse spin current in magnetic nanowires. *Physical Review B* 87, 22 (2013), 224402.
- [16] LANDAU, L., AND LIFSHITZ, E. On the theory of the dispersion of magnetic permeability in ferromagnetic bodies. *Phys. Z. Sovietunion* 8 (1935), 153–169.
- [17] MELCHER, C. The logarithmic tail of Néel walls. *Arch. Ration. Mech. Anal.* 168, 2 (2003), 83–113.
- [18] MELCHER, C. Domain wall motion in ferromagnetic layers. *Phys. D* 192, 3-4 (2004), 249–264.
- [19] MELCHER, C. Thin-film limits for Landau-Lifshitz-Gilbert equations. *SIAM J. Math. Anal.* 42, 1 (2010), 519–537.
- [20] MELCHER, C. Global solvability of the cauchy problem for the Landau-Lifshitz-Gilbert equation in higher dimensions. *Indiana Univ. Math. J.*, to appear (2011).
- [21] MELCHER, C., AND PTASHNYK, M. Landau-Lifshitz-Slonczewski equations: global weak and classical solutions. *SIAM J. Math. Anal.* 45, 1 (2013), 407–429.
- [22] MEYRIES, M., RADEMACHER, J. D., AND SIERO, E. Quasilinear parabolic reaction-diffusion systems: user’s guide to well-posedness, spectra and stability of travelling waves. *submitted, ArXiv 1305.3859*.

- [23] PODIO-GUIDUGLI, P., AND TOMASSETTI, G. On the evolution of domain walls in hard ferromagnets. *SIAM J. Appl. Math.* 64, 6 (2004), 1887–1906 (electronic).
- [24] SLONCZEWSKI, J. C. Current-driven excitation of magnetic multilayers. *Journal of Magnetism and Magnetic Materials* 159, 11 (1996), L1–L7.